

Full Paper

Development of an Admittance Sensor for Isoniazid using Differential Coulometric FFT Admittance Voltammetry in a Flow Injection Analysis System

Mehrnaz Ebrahimi,¹ Parviz Norouzi^{1,2*} and Bagher Larijani^{3*}

¹*Center of Excellence in Electrochemistry, School of Chemistry, College of Science, University of Tehran, Tehran, Iran*

²*Biosensor Research Center, Endocrinology & Metabolism Molecular-Cellular Sciences Institute, Tehran University of Medical Sciences, Tehran, Iran*

³*Endocrinology & Metabolism Research Center, Endocrinology & Metabolism Molecular-Cellular Sciences Institute, Tehran University of Medical Sciences, Tehran, Iran*

*Corresponding Author, Tel.:+98-216112294

E-Mail: norouzi@khayam.ut.ac.ir; emri@tums.ac.ir

Received: 5 April 2017 / Received in revised form: 15 May 2017 /

Accepted: 18 May 2017 / Published online: 30 September 2017

Abstract- In this work, for the first time, a new electrochemical detection system for Isoniazid was developed using combination of modified carbon paste electrode with Coulometric fast Fourier transformation admittance voltammetry (CFFTAV). The sensor was fabricated by using graphite powder, SiC nanoparticles and ionic liquid (CILSiCE), and casting reduced graphene oxide, ionic liquid, SWCNT, and gold nanoparticles. This electrode was characterized by SEM and electrochemical impedance spectroscopy methods. In the optimal conditions, the electrode exhibited a linear response to Isoniazid from 0.5 to 300 nM and detection limit was 0.15 nM. Moreover, the proposed sensor exhibited good accuracy and repeatability (R.S.D value of 2.45%) and long term stability, up to 70 days with a decrease of 4.1% in the response. The proposed method was used to the determination of Isoniazid in real samples, successfully.

Keywords- FFT Admittance Voltammetry, Isoniazid, Gold nanoparticles, Graphene, SWCNT

1. INTRODUCTION

Isoniazid (INI), is known as anti-tuberculosis drug that has been used for chemotherapy of tuberculosis, which may induce hepatotoxicity and sometimes even cause death, when repeated use of the drug [1,2]. Hence, for effective therapeutic dosages, it is need to measure INI level in biological liquid [3]. Fig. 1 shows the two and three dimensional structure of the INI. There are a numerous analytical methods for measurement of INI in biological concentration levels [4-7]. Among them, the electrochemical (EC) methods, that have been proven to be sensitive and reliable for the determination of electroactive drug components, are used more common for INI measurement in pharmaceutical dosage forms and biological fluids. In this direction, various voltammetry techniques at with solid electrodes, such as Au, Pt and carbon based electrode (GCE), have been used [8-13].

The voltammetry of INI at bare glassy carbon electrode (GCE), shows of a peak with high overpotentials (>900 mV), due to the direct oxidation. For this reason, the measurement has a low sensitivity and selectivity. Therefore, it is necessary to develop new modified GC electrodes, with nanoparticles (NPs) for obtaining higher sensitive measurement of INI [8,9,12].

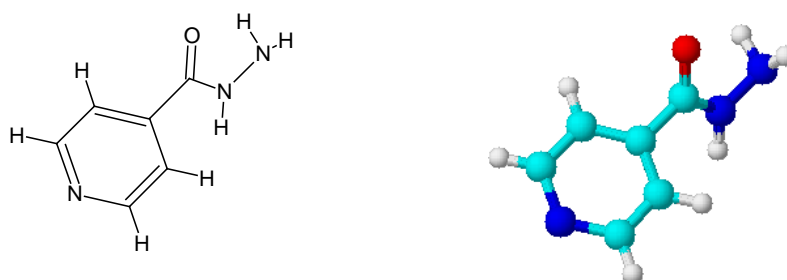


Fig. 1. Two and three dimensional chemical structure of Isoniazid

The carbon nanostructures, with special electrochemistry, are the most dynamic and developing nano-size substances in modification of electrodes. Existing a great number of publications with graphene, bamboo-like, multi-walled, double-walled and single walled carbon nanotubes are the evidence for their importance [14-16]. For example, graphene with its various derivatives, due to its notable electrochemical properties, has shown attractive advantages in construction of sensors, such as electrochemical devices, capacitors, or transistors [16]. Furthermore, it will be attractive to prepare graphene-based hybrid composites with CNT or noble metal, because such materials may generate synergy effect and thus enhance their performance in sensing applications [17]. For instance, combination of Au NPs and carbon nanostructures with various EC techniques, as developed new sensors, have been widely used as a sensitive detection of compounds [18-20]. Specifically, Au NPs has interested of experts due to its large specific surface area, easy employment and recovery and have presented their interesting respects in graphene [21].

The present work reports a new electrochemical system based on the combination of coulometric FFT admittance voltammetry (CFFTAV) technique [22-24] with a new sensor and flow injection analysis. The sensor consisted of graphite powder, SiC NPs and ionic liquid, which was modified by casting graphene oxide, ionic liquid, SWCNT, and gold NPs. The sensor was characterized by SEM and electrochemical impedance spectroscopy (EIS) methods. The presence of nanomaterial in the matrix of the sensor can enhance the sensitivity of the measurements. In the optimal conditions, the electrode exhibited a linear response to INI.

2. MATERIALS AND METHODS

2.1. Reagents

Isoniazid was purchased from Sigma–Aldrich. 1-ethyl-3-methylimidazolium tetrafluoroborate (EMIMBF₄, IL) were of analytical grades. All other chemicals were analytical grade form Merck Co., and are used without further purification. Double distilled water was used throughout. The prepared solutions were kept at 4 °C before use.

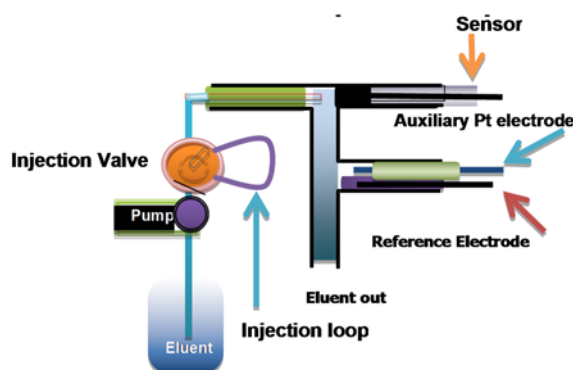


Fig. 2. The diagram of the electrochemical cell used in flow injection analysis

2.2. Electrochemical System

A homemade potentiostat was used for admittance voltammetric measurements, which was interfaced to a PC equipped by using an analog to digital (A/D) data acquisition board (PCL-818H, Advantech Co.). An electrochemical program software was developed for generating the potential waveform, which was continuously applied to the working electrode, and data acquisition requirements. The program was, also used to process and plot the data in real time. Also, for flow injection analysis, the equipment was integrated with an eight roller peristaltic pump (UltrateckLabs Co., Iran) and a four way injection valve (Supelco Rheodyne Model 5020) with 300 μ L sample injection loop [25-29].

A stock solution of 2 mM INI was firstly prepared, and then an aliquot was diluted to the appropriate concentration. The INI solutions were introduced into the sample loop by a plastic syringe. A three-electrode configuration was employed in all experiments, with potentials referring to an Ag/AgCl as the reference electrode, and a Pt electrode (2.0 mm in diameter) as auxiliary electrode in the flow cell (see Fig. 2). The electrochemical measurements were evaluated by CFITAV method. EIS measurements were performed in 0.5 mM $K_3Fe(CN)_6$ in PBS at pH 7.4.

2.3. Sensor preparation

The based electrode was carbon paste ionic liquid SiC electrode (CILSiCE, which was a mixture of 0.3 mL of EMIMBF₄, liquid paraffin, 4.0 g of graphite powder and 40 mg of SiC NPs in a mortar and heated to form a homogeneous carbon paste. The paste was packed into a cavity of Teflon tube (i.d. 3.1 mm), then, an electrical contact was established via a copper wire to the paste in the inner hole of the tube.

Primarily, graphene oxide was synthesized using the Hummer's method with slight modification [30]. In brief, graphene nanosheets oxide (GNO) was synthesized from graphite through oxidization using NaNO₃, H₂SO₄, and KMnO₄. Next, a 1.0 mg/mL solution was ultrasonicated for 1.5 h to form a clay bank dispersion and was further reacted with 7.0 mL of hydrazine hydrate for 12 h under 95 °C. Reduced graphene nanosheets (RGNS) was filtrated, collected by and further washed with water.

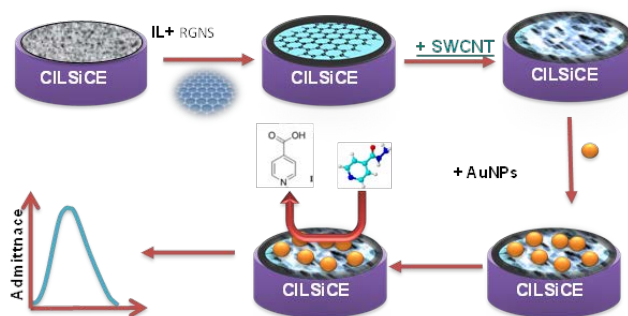


Fig. 3. Schematic of the sensor preparation

The fabrication of AuNPs/SWCNT/RGNS-IL/CILSiCE involves following stages. 0.1-0.8 mg of RGNS and EMIMBF₄ (20 μ L) were dispersed in 2.0 ml dimethylformamide (DMF) with the aid of ultrasonic agitation to achieve a well-dispersed suspension. Then, 20 μ L of the suspension was dropped on a cleaned CILSiCE to form RGNS-IL/CILSiCE electrode and let the solvent to evaporate in air. Then, SWCNT (1.0 mg/mL in H₂O) was subjected to mild ultra-sonication for 5 min before use. Afterward, 8.0 μ L of the solution was applied on the surface of the RGNS-IL/CILSiCE and kept in isolating container until completely dried. At

that point, a 4 ml 1.0% HAuCl₄ solution was added and stirred for 30 min again. Finally, for obtaining AuNPs/SWCNT/RGNS-IL/CILSiCE, the electrochemical deposition of Au NPs was performed in 0.2 M Na₂SO₄ aqueous solution of HAuCl₄ (1.0 mM) with the applied potential of -0.20 V.

3. RESULTS AND DISCUSSION

The surface morphology of the AuNPs/SWCNT/RGNS-IL/CILSiCE was examined by SEM. As shown in Fig. 4A, it can be seen that the SWCNT layer exhibits a morphology consisting of a network-like structure without aggregation that is, so far, evenly covered the surface of the electrode. It also illustrates the magnitude and distribution of Au NPs on the surface of AuNPs/SWCNT/RGNS-IL/CILSiCE, which are almost, uniform. The morphology and size distribution of electrodeposited Au NPs on SWCNT/RGNS-IL can be controlled by electrodeposition parameters, such as electrodeposition time and the concentration of the plating solution.

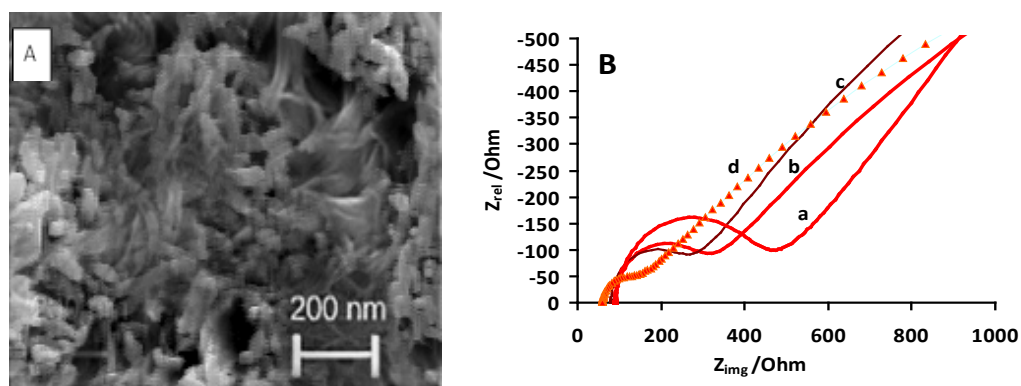


Fig. 4. (A) SEM image of AuNPs/SWCNT/RGNS-IL/CILSiCE; (B) EIS of (a) bare CILSiCE, (b) RGNS-IL/CILSiCE, (c) SWCNT/RGNS-IL/CILSiCE, and (d) AuNPs/SWCNT/RGNS-IL/CILSiCE in the solution of 3 mM Fe(CN)₆^{4- / 3-}

EIS is known as an effective method to study the interface properties of modified electrodes. In which, a semicircle locates at high frequencies, which corresponds to the charge transfer resistance (R_{ct}), and a line at low frequencies resulting from the diffusion limiting step. Also, the value of R_{ct} is related to the conductivity of the modified surface. Fig. 4B demonstrates the results of EIS measurements at different stages of the sensor fabrication process, in 3.0 mM [Fe(CN)₆]^{3-/4-} in 0.1 M KCl. It can be seen in curve (a) for the bare CILSiCE that the value of R_{ct} is around 480 ohm. But in case of RGNS-IL/CILSiCE (curve b), the change in the value of R_{ct} (363 ohm) indicates the RGNS-IL could not enhance the conductivity of the composite film. However, curve (c) shows that the addition of SWCNT to the surface, decreased the value of R_{ct} to value of 300 ohm. These points to that combination

of SWCNT and RGNS-IL could enhance their synergistic effect and electrical conductivity of surface. For the same reason, addition of Au NPs (curve d) cause the value of R_{ct} decreased significantly and reaches to 175 ohm.

Fig. 5 illustrates the cyclic voltammograms (CVs) of different electrodes in 3 mM $K_3Fe[CN]_6$ and 0.5 M KCl mixture solution. On bare CILSiCE (curve a), a pair of define redox peaks appeared with the smallest redox peak currents and the peak-to-peak separation (ΔE_p) was calculated as 380 mV. On RGNS-IL/CILSiCE (curve b), the redox peak currents increased and the ΔE_p value decreased to 300 V, which indicated that the electron transfer was enhanced. Alike, on SWCNT/RGNS-IL (curve c), the redox peak currents also changed with the ΔE_p value (230 mV), may due to existence of a higher surface area and conductivity of the film on the electrode surface. For AuNPs/MWCNT/RGNS-IL/CILSiCE electrode (curve d), the biggest redox peak currents

Appeared with the smallest ΔE_p value as 100 V, which was almost the close to the theoretical value of 59 mV for the redox probe of $[Fe(CN)_6]^{3-/4-}$. The results could be attributed to the synergistic effects of the existing nanomaterials in the composites on the electrode surface.

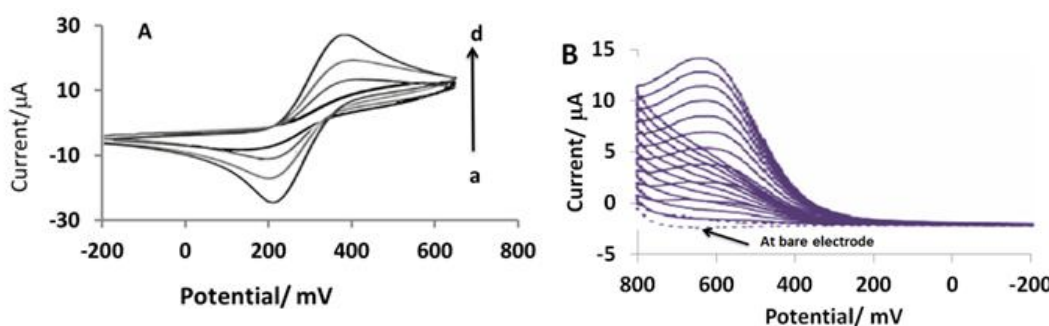


Fig. 5. A) Cyclic voltammograms of 3.0 mM $[Fe(CN)_6]^{3-/4-}$ in 0.5 mol/L KCl recorded at (a) CILSiCE, (b) RGNS-IL/CILSiCE, (c) SWCNT/RGNS-IL/CILSiCE, and (d) AuNPs/SWCNT/RGNS-IL/CILSiCE; B) The electrochemical oxidation of 2.0×10^{-7} M INI in PBS (pH 6.5) on bare electrode (dash), and AuNPs/SWCNT/RGNS-IL/CILSiCE electrode at scan rates 20, 40, 60, 80, 100, 120, 140, 160, 180, 200 mV/s

The electrochemical oxidation of INI on AuNPs/SWCNT/RGNS-IL/CILSiCE at different scan rates was examined in PBS (pH 6.5) containing 2.0×10^{-7} M of INI. As the CV curves in Fig. 5B show, there is an irreversible anodic peak at 590 mV. It should be mentioned that peak current of the anodic peak is almost 2.5 times higher along with decrease in oxidation over potential than that observed at the bare CILSiCE (dash curve in Fig 5B). The improvement in the INI peak current is attributed to the electrocatalytic effect of the

composite nanoparticles on the electrode surface processes. Also, the oxidation peak currents increased linearly with shifts in the peak potentials toward positive directions upon increasing the scan rates from 20 to 200 mV s⁻¹. The corresponding linear regression ($r^2=0.994$) equation can be expressed as follows:

$$I_{pa}=0.43 (v^{1/2}/mV/s)+ 5.70 \quad (1)$$

3.1. Analytical performance of the sensor

To improve the sensitivity of the electrochemical system \ a flow injection analysis has been used in combination with coulometric FFT admittance voltammetry (CFFTAV) technique [31-34]. Fig. 6 showed the differential admittance voltammograms recorded during CFFTAV INI measurement, by the sensor in PBS at pH 6.5. The time axis represents the time passing between the beginnings of the experiment and ending of the potential scan (i.e. it represents a number of the scans). In this measurement, the SW pulse had amplitude of 25 mV and a frequency of 200 Hz in the potential range of 0 to 700 mV.

One important advantageous in CFFTAV is to collect eight current samples in the forward and reverse SW pulses [35]. It must also be mentioned that in this graph the reference admittance voltammogram was subtracted from the subsequent voltammograms, based on this equation,

$$\Delta A= A_i-A_r \quad (2)$$

Where, the reference admittance, A_r , is obtained by averaging admittance, A_i , of 5 voltammograms at the beginning of the experiment. The figure shows that the before an injection of solution, there is no changes in the voltammograms. However, by the injection of 300 μ L of 5.0×10^{-7} M INI, in the PBS at pH 6.5, a signal appears in differentiate admittance voltammogram.

The sensor response is calculated based on the admittance integration in a potential range. Here the total absolute difference charge ΔQ can be determined by the following equation:

$$\Delta Q = Q - Q_0 \quad (3)$$

Where Q is the electrical charge obtained by integration of voltammetric curves between 0 and 700 mV, and Q_0 represents the value of Q in the absence of the analyte. The measurement of a set of standard solutions point out that the value of ΔQ was proportional to the INI concentration in the injected samples. By optimizing experimental parameters the ΔQ response can be maximized.

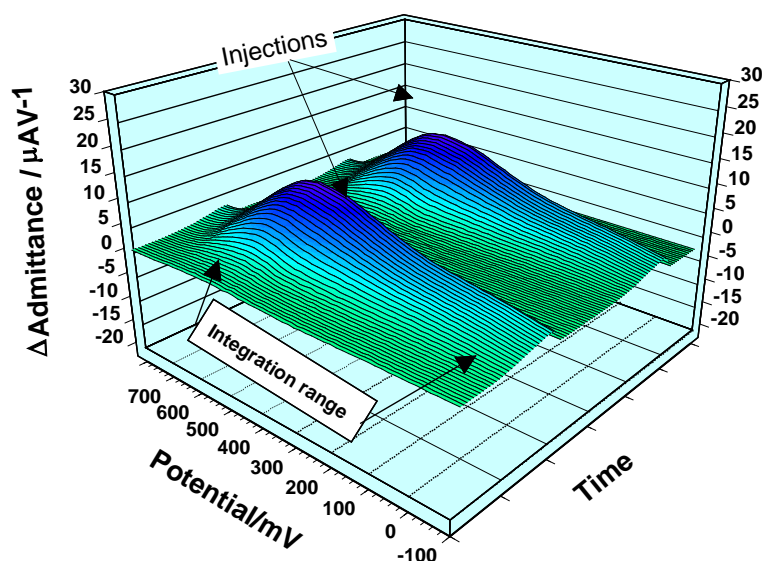


Fig. 6. a) Differential FFT admittance voltammograms of AuNPs/SWCNT/RGNS-IL/CILSiCE sensor in absence and with injection of 5.0×10^{-7} M INI in PBS at pH 6.5 in the potential range of 0 to 700 mV at SW frequency 200 Hz and amplitude 25 mV in PBS at pH 6.5

3.2. Optimization frequency and amplitude

In the SW voltammetric methods, the sensitivity of the electrochemical system is associated to the SW frequency and amplitude of the exciting potential waveform. Consequently, in order to gain maximum ΔQ , it is need to find the optimum condition of the waveform in the electrode response. Therefore, the electrode response was measured at the SW frequency range from 50 to 550 Hz and amplitude from 5 to 40 mV. Fig. 7 demonstrates the electrode response in solution of 5.0×10^{-7} M of INI and PBS at pH 6.5, at those frequencies and amplitudes.

The electrode reopens amplifies with the SW frequencies up 200 Hz. However, using lower SW frequencies reduce the current peak value, similar to the current decline in application of a small scan rate in CV method. This can, also, lead to use a longer time used for the potential scanning, which result to lower number of potential scan for each injected sample zone. Under this condition the value of ΔQ drops.

On the other hand, the SW results shows at frequencies higher than 200 Hz, in which a potential scan take place in a shorter time, the response peak becomes smaller. One possible reason for this is the kinetic limitation of the EC processes at the sensor surface, where there is no adequate time for the diffusion or electron transfer of the analyte. Also, at very high frequencies, the response decline is higher due to the solution resistance, electrode diameter, and stray capacitance of the system. For the same reasons, the results, also, show that the optimal amplitude for the determination of INI is 25 mV.

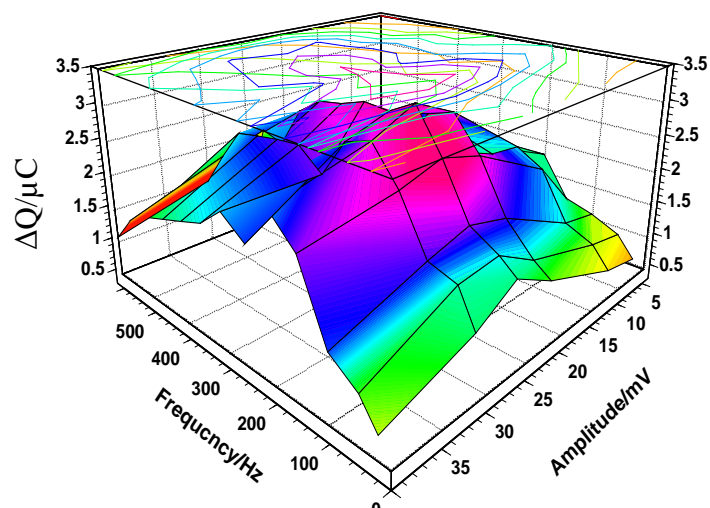


Fig. 7. The effect of frequency and amplitude of SW on the CFFTAV response of AuNPs/SWCNT/RGNS-IL/CILSiCE sensor to the injection of 5.0×10^{-7} M INI solution, the potential integration range for the admittance was 0-700 mV

3.3. Optimization of pH

The effect of pH on the response of INI at the sensor surface was tested in various buffer solutions. Fig. 8 shows the change in ΔQ for the solution of 5.0×10^{-7} M of INI at frequency of 200 Hz and amplitude of 25 mV. As shown, the sensor response at first increases with pH up to 6.5, and then decreased by going to higher pHs.

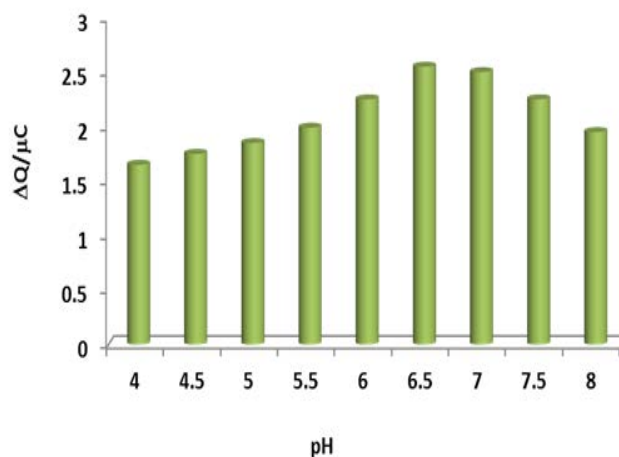


Fig. 8. The effect of pH on sensor response for the solution of 5.0×10^{-7} M of INI, recorded at SW frequency of 200 Hz and amplitude of 25 mV in PB solution, and the potential integration range for the admittance was 0 to 700 mV

Observing such behavior for the electrode response could be attributed to the change in the nature and the charge of the drug molecule in various pHs, where the interactions between the drug and the electrode surface. The linear regression equation between the reduction peak

potential and pH had a slope of -54 mV/pH unit, which is indicating that the equal amounts of electrons and protons involved in the electrode reaction (i.e. two electron-two proton process).

3.4. Calibration curve and sensor characterization

For determination the sensitivity and detection limit of the electrochemical system, the change of the sensor response, ΔQ , with concentration of INI was studied. As mentioned above, the value of the response was depended to the choice of the potential integration range. For this reason, ΔQ was calculated based on equation 2 in potential range 0 to 700 mV to gain maximum value for the response. Fig. 9 demonstrates the calibration curve for AuNPs/SWCNT/RGNS-IL/CILSiC electrode in INI standard solutions from 2 nM to 400 nM at pH 6.5, under optimized experimental conditions. The inset A, in Fig. 9 shows coulometric Q-t response of the sensor to injections of INI standard solutions into a flowing supporting electrolyte, PBS pH 6.5. As shown, after each injection of INI solution ΔQ increased immediately and reached to steady state. The injection was done with a regular time interval, and the complete signal recovery was achieved for the successive injections, which verifies the absent of memory effect.

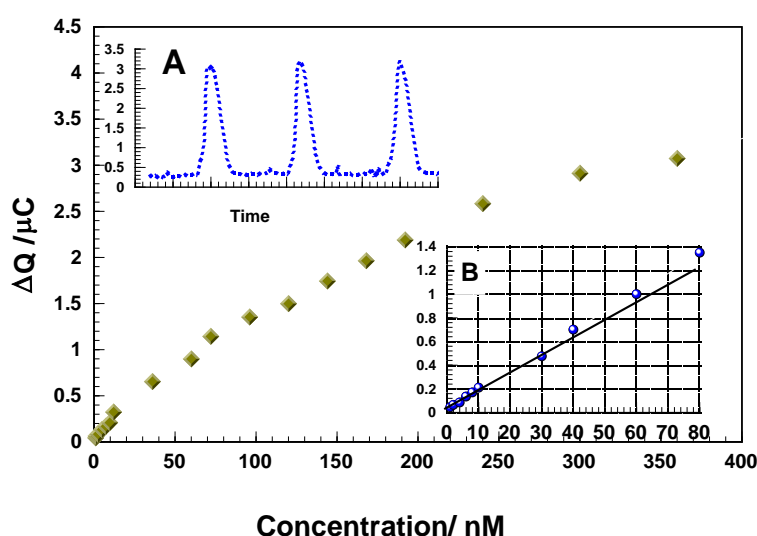


Fig. 9. The calibration curve for AuNPs/SWCNT/RGNS-IL/CILSiC in INI M determination PBS at pH 6.5 in the potential range of 0 to 700 mV at SW frequency 200 Hz and amplitude 25 mV in PBS at pH 6.5, A) Coulometric Q-t curve for injection of INI into flowing supporting electrolyte, PBS pH 6.5, the potential integration range for the admittance was 0 to 700 Mv; B) The linear part of calibration curve

Fig. 9 inset B, displays the linear section of the calibration curve in the concentration range from 0.02 to 80.00×10^{-9} M, which leads to the estimation of the detection limit and the

linearity by linear regression analysis. The regression equation was $\Delta Q=0.44C+0.088$ with a correlation coefficient of 0.992, and the detection limit was estimated to be 0.15 nM, based on a signal to noise ratio of 3.

To evaluate the performance of AuNPs/SWCNT/RGNS-IL/CILSiC sensor in real sample, a similar procedure was also used for INI in commercial tablets (100 mg/tablet INI). INI stock solution with concentration of 1.0×10^{-3} M was prepared as mentioned in the experimental part. Then, standard addition of INI in the stock solution was injected, and the data were calculated from five replicates. Table 1 shows the data generated by standard addition method for the analysis of INI in buffer solution of pH 6.5.

Table 1. Recovery data obtained by standard addition method for INI in drug formulation

Formulation	Tablets/(ng/mL)	Added (ng/mL)	Found (ng/mL)	Recovery (%)
INI	7.1	5.00	12.24	99.4
	45.5	5.00	50.10	100.1
	86.2	5.00	91.20	100.2
	110.8	5.00	114.92	99.8

The detection limit of the AuNPs/SWCNT/RGNS-IL/CILSiC sensor was compared with some of the best previously reports for INI detection (Table 2). Those data confirms that the presented electrochemical detection system could demonstrate a good and reproducible sensitivity [8,11-13].

Table 2. The comparison of AuNPs/SWCNT/RGNS-IL/CILSiC INI sensor with the best previously reported INI determination methods based on different detection techniques

Detection Method	Materials	DL (nM)	Ref.
Amperometry	Nf/Fe(tmphen) ₃ ²⁺ modified GCE	13×10^3	[8]
DPV	MWCNT–chit) modified GCE	50	[11]
DPV	Poly(amidosulfonic acid) modified GCE	10	[12]
LSV	ERGO modified GCE	17×10^3	[13]
CFFTAV	AuNPs/SWCNT/RGNS-IL/CILSiC	0.15	This work

3.5. Stability and reproducibility

Reproducibility and stability are the most important parameters for quality of the constructed electrochemical sensor. For this reason, the measurements were repeatedly performed 5 times with a single sensor in the solution containing 0.5 μ M of INI. The relative

standard deviation (RSD) of the oxidation current is found to be 2.45%, which shows a good reproducibility. Operational stability of the suggested sensor is tested 70 days, and it shows a decrease about 4.1% in the initial response.

4. CONCLUSIONS

An ultra-sensitive INI electrochemical system has been developed by using AuNPs/SWCNT/RGNS-IL/CILSiCE and CFFTA voltammetry in flow injection analysis. This setup was successively employed to calculate the electrode response in form of ΔQ , in a selected potential range by integrating the admittance. Also, the sensor exhibited good analytical characteristics, such as higher affinity towards INI, with a good repeatability and reproducibility. Hence, this combined electrochemical system has shown an acceptable and promising performance for sensitive determination of drugs, which can be considered a very effective approach for probing the characteristics of new surface modified electrode.

Acknowledgement

The authors are grateful to the Research Council of University of Tehran for the financial support of this work.

REFERENCES

- [1] S.Chouchane, I. Lippai, and R. S. Magliozzo, *Biochemistry* 39 (2000) 9975.
- [2] M.Sievers, and R. Herrier, *Am. J. Health-System Pharm.* 32 (1975) 202.
- [3] J. A. Romero, and F. J. Kuczler Jr, *Am. Family Physician* 57 (1998) 749.
- [4] A. Hutchings, R. Monie, B. Spragg, and P. Routledge, *J. Chromatog. B* 277 (1983) 385.
- [5] J. W. Jenne, *Am. Rev. Respirat. Disease* 81 (1960) 1.
- [6] S. H. Song, S. H. Jun, K. U. Park, Y. Yoon, J. H. Lee, J. Q. Kim, and J. Song, *Rapid Commun. Mass Spectromet.* 21 (2007) 1331.
- [7] B. Haghighi, and S. Bozorgzadeh, *Microchem. J.* 95 (2010) 192.
- [8] U. P. Azad, and V. Ganesan, *J. Solid State Electrochem.* 16 (2012) 2907.
- [9] U. P. Azad, N. Prajapati, and V. Ganesan, *Bioelectrochemistry* 101 (2015) 120.
- [10] M. M. Ghoneim, K. Y. El-Baradie, and A. Tawfik, *J. Pharm. Biomed. Anal.* 33 (2003) 673.
- [11] S. Shahrokhian, and M. Amiri, *Microchim. Acta* 157 (2007) 149.
- [12] G. Yang, C. Wang, R. Zhang, C. Wang, Q. Qu, and X. Hu, *Bioelectrochemistry* 73 (2008) 37.
- [13] S. Cheemalapati, S. Palanisamy, and S. M. Chen, *Int. J. Electrochem. Sci.* 8 (2013) 3953.

- [14] C. Gómez-Navarro, R. T. Weitz, A. M. Bittner, M. Scolari, A. Mews, M. Burghard, and K. Kern, *Nano Lett.* 7 (2007) 3499.
- [15] J. J. Gooding, *Electrochim. Acta* 50 (2005) 3049.
- [16] M. Zhou, Y. Zhai, and S. Dong, *Anal. Chem.* 81 (2009) 5603.
- [17] X. Huang, X. Qi, F. Boey, and H. Zhang, *Chem. Soc. Rev.* 41 (2012) 666.
- [18] T. T. Baby, S. S. J. Aravind, T. Arockiadoss, R. B. Rakhi, and S. Ramaprabhu, *Sens. Actuators B* 145 (2010) 71.
- [19] W. Hong, H. Bai, Y. Xu, Z. Yao, Z. Gu, and G. Shi, *J. Phys. Chem. C* 114 (2010) 1822.
- [20] C. Shan, H. Yang, D. Han, Q. Zhang, A. Ivaska, and L. Niu, *Biosens. Bioelectron.* 25 (2010) 1070.
- [21] M. C. Daniel, and D. Astruc, *Chem. Rev.* 104 (2004) 293.
- [22] V. K. Gupta, P. Norouzi, H. Ganjali, F. Faridbod, and M. Ganjali, *Electrochim. Acta* 100 (2013) 29.
- [23] P. Norouzi, V. K. Gupta, B. Larijani, S. Rasoolipour, F. Faridbod, and M. R. Ganjali, *Talanta* 131 (2015) 577.
- [24] P. Norouzi, B. Larijani, M. Ganjali, and F. Faridbod, *Int. J. Electrochem. Sci.* 9 (2014) 3130.
- [25] P. Norouzi, M. R. Ganjali and L. Hajiaghababaei, *Anal. Lett.* 39 (2006) 1941.
- [26] P. Norouzi, G. R. Nabi Bidhendi, M. R. Ganjali, A. Sepehri and M. Ghorbani, *Microchim Acta* 152 (2005) 123.
- [27] P. Norouzi, M. R. Ganjali, A. Sepehri and M. Ghorbani, *Sens. Actuators B-Chem* 110 (2005) 239.
- [28] P. Norouzi, M. R. Ganjali, M. Zare and A. Mohammadi, *J. Pharm. Sci.* 96 (2007) 2009.
- [29] P. Norouzi, M. R. Ganjali and P. Matloobi, *Electrochem. Commun.* 7 (2005) 333
- [30] J. Chen, B. Yao, C. Li, and G. Shi, *Carbon* 64 (2013) 225.
- [31] P. Norouzi, I. Alahdadi, and S. J. Shahtaheri, *Int. J. Electrochem. Sci.* 10 (2015) 3400.
- [32] P. Norouzi, M. R. Ganjali, and A. E. Meibodi, *Anal. Lett.* 41 (2008) 1208.
- [33] P. Norouzi, B. Larijani, F. Faridbod, and M. R. Ganjali, *Int. J. Electrochem. Sci.* 8 (2013) 6118.
- [34] P. Norouzi, B. Larijani, M. Ganjali, and F. Faridbod, *Int. J. Electrochem. Sci.* 7 (2012) 10414.
- [35] P. Norouzi, V. K. Gupta, F. Faridbod, M. Pirali-Hamedani, B. Larijani, and M. R. Ganjali, *Anal. Chem.* 83 (2011) 1564.